INTERNATIONAL SYMPOSIUM ON GLASS SCIENCE & TECHNOLOGY

October 6-8, 1993
Athens, Greece

Organized by the
HELLENIKOS HYALOURGIKOS SYNDESMOS
(Greek Glass Federation)

Under the auspices of the
INTERNATIONAL COMMISSION ON GLASS

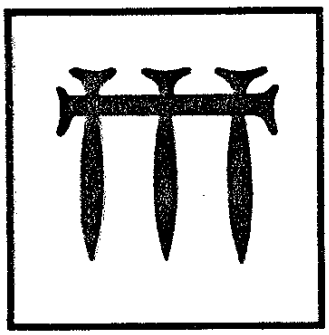

Proceedings of the

INTERNATIONAL SYMPOSIUM ON GLASS SCIENCE AND TECHNOLOGY

Athens, 6-8 October 1993

Editors: G. D. Chryssikos and E. I. Kamitsos

Chimica Chronica, New Series, 23, 335-340 (1994)

RAMAN AND FAR-INFRARED STUDY OF ALUMINUM AND BORON SUBSTITUTED SODIUM TRISILICATE GLASS

E. I. Kamitsos and J. A. Kapoutsis
Theoretical and Physical Chemistry Institute,
National Hellenic Research Foundation,
48 Vas. Constantinou Ave.,
116 35 Athens, Greece

H. Jain and C. H. Hsieh
Department of Materials Science and Engineering,
Lehigh University, Bethlehem, PA 18015, USA

The structure of glasses in the system $Na_2O.xR_2O_3.(3-2x)SiO_2$ (R=Al, B) has been studied by employing Raman spectroscopy. The purpose of this work is to elucidate the role of aluminum and boron substitution on glass structure and properties while keeping the Na/(Si+R) ratio fixed. Aluminum was found to enter the silicate network and occupy Q^3 sites, causing the equilibrium $2Q^3 \rightleftharpoons Q^4+Q^2$ to shift to the left. The role of boron was found to be opposite, since it induces the destruction of Q^3 species in favour of the highly charged Q^1 and Q^2 species and the fully polymerized Q^4 silicate units.

INTRODUCTION

The influence of boron and aluminum substitution for silicon on the properties of silicate glasses is well known (1, 2). Of particular interest is the behaviour of ionic conductivity, which increases when Al_2O_3 substitutes for SiO_2, but decreases when B_2O_3 is added to the silicate glass (3-5). Aluminum and boron have, therefore, the opposite effect on ionic conductivity, regardless of the fact that both trivalent ions are thought to behave as network formers in silicate glasses (3-6).

To elucidate the origin of such different effects of Al and B we have undertaken a Raman study of sodium-aluminosilicate (SAS) and sodium-borosilicate (SBS) glasses of the general formula $Na_2O.xR_2O_3.(3-2x)SiO_2$ (R=Al, B). This compositional variation was chosen to maintain a constant network modifier (Na) to network former (Si+R) ratio, while SiO_2 is gradually replaced by Al_2O_3 or B_2O_3. The far-infrared spectra were also measured to investigate the interactions between sodium ions and their sites in the glass, which are relevant to ion conduction properties. Results of this investigation are reported in this work.

EXPERIMENTAL

SAS (x=0, 0.2, 0.4, 0.6) and SBS (x=0, 0.2, 0.4, 0.6, 0.8, 1.0) glasses were prepared by melting stoichiometric mixtures of reagent grade Na_2CO_3, H_3BO_3, Al_2O_3 and SiO_2 and subsequent quenching into a stainless steel mold. Melting temperatures in the range 1100-1640°C were required, depending on composition. Details on glass preparation can be found elsewhere (6). SAS glasses with x=0.8 and 1.0 could not be prepared with sufficient homogeneity due to the high viscosity of the melt.

Raman spectra were recorded on a Ramanor HG 2S Jobin-Yvon spectrometer coupled to a PC for data acquisition and analysis. Excitation was provided by the 488.0 nm line of a Spectra Physics 165 argon ion laser (500 mW at 90° geometry). To reveal clearly the low-frequency Raman scattering (<200 cm^{-1}) the temperature-reduced Raman intensity, I_{red}, was calculated by

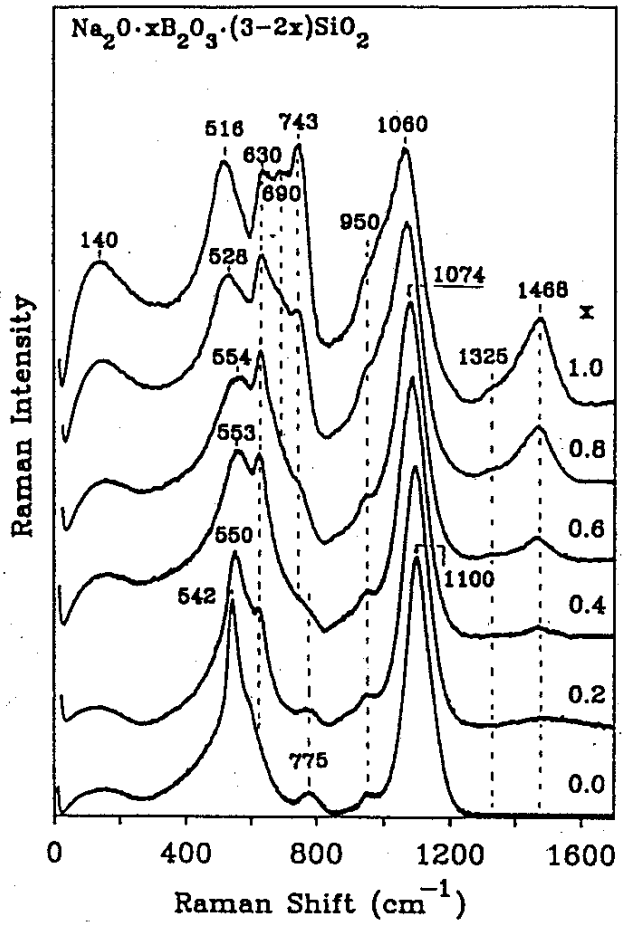

Fig. 1. *Raman spectra of SBS glasses*

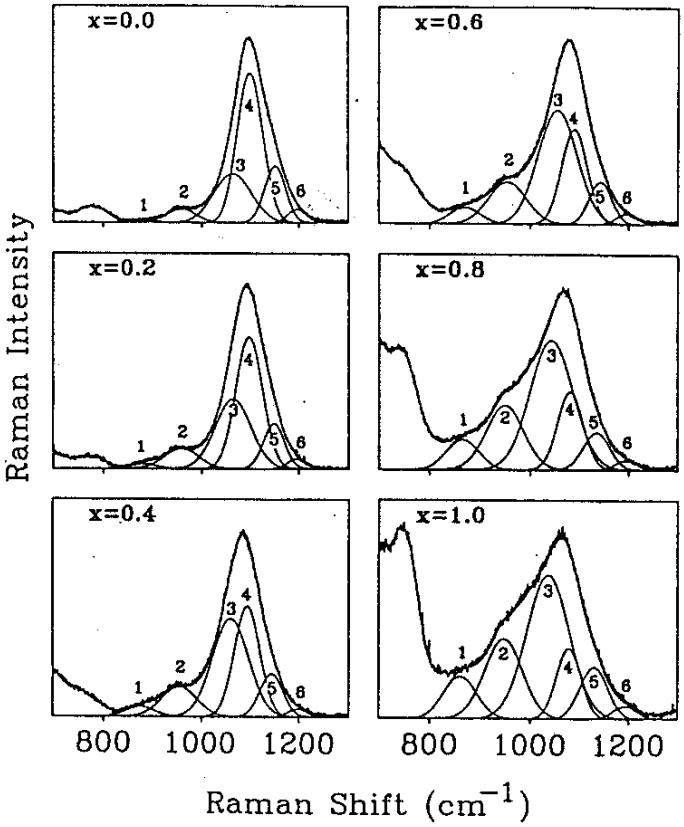

Fig. 2. *Deconvolution of the 800-1200 cm^{-1} profiles of the Raman spectra of SBS glasses.*

$$I_{red}=I(\nu)/(1+n(\nu)) \quad (1)$$

where I(ν) is the measured Raman intensity and n(ν) is the Bose-Einstein distribution factor,

$$n(\nu)=[\exp(hc\nu/k_BT)-1]^{-1} \quad (2)$$

where ν is the Raman shift (cm^{-1}), c is the speed of light, T is the temperature and k_B and h are the Boltzmann and Planck constants, respectively.

Infrared spectra were measured in the reflectance mode (11° off-normal) on a Fourier-transform spectrometer (Bruker 113v). The reflectance data were analysed by the Kramers-Kronig transformation method to obtain the absorption coefficient spectra reported in this work.

RESULTS AND DISCUSSION

The Structure of Sodium-Borosilicate Glasses

The Raman spectra of SBS glasses are shown in Fig. 1. Replacement of Si by B induces systematic spectral variations, which imply corresponding structural changes. In the low frequency range new bands develop at 630, 690 and 743 cm^{-1} as x increases. Bands in the region 400-700 cm^{-1} have been attributed to a delocalized vibration of Si-O-Si bridges; this mode having a mixed stretching-bending character (7-9). The frequency of this mode increases

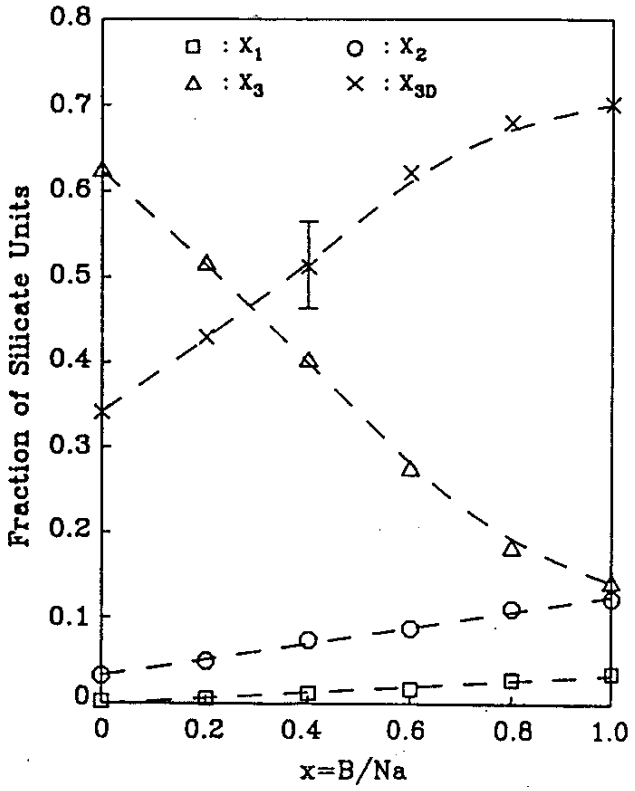

Fig. 3. *Effect of boron substitution for silicon on the relative abundance of silicate tetrahedra in SBS glasses.*

as the degree of silicate network depolymerization increases, i.e. upon decreasing the number of bridging oxygen atoms per silicon tetrahedron Q^i (i= number of bridging oxygen atoms). Based on the results of previous Raman studies of silicate glasses we assign the band at 630 cm^{-1} to Si-O-Si bridges between Q^2 species and the one at 690 cm^{-1} to Si-O-Si bridges between Q^1 species. Thus, it appears that the presence of boron favours the formation of Q^2 and Q^1 silicate tetrahedra.

Borate centers are present mainly in the form of $B\mathcal{O}_4^-$ tetrahedra ($\mathcal{O}$= bridging oxygen atom), as well as $B\mathcal{O}_2O^-$ triangles. Evidence for $B\mathcal{O}_4^-$ tetrahedra is provided by the band at 743 cm^{-1} which develops at high B/Si ratios. Bands at similar frequencies in the spectra of alkali borate glasses have been attributed to six-membered borate rings containing $B\mathcal{O}_4^-$ tetrahedra (10). The asymmetric envelope developing in the region 1300-1600 cm^{-1} is indicative of the formation of $B\mathcal{O}_2O^-$ borate triangles, since the localized stretching vibration of their $B\text{-}O^-$ bonds is active in this frequency range (10).

Of particular interest is the effect of boron substitution on the 800-1250 cm^{-1} envelope, which appears to broaden and downshift upon increasing the boron content. Bands in this frequency range of the Raman spectra of modified silicate glasses originate from the overlapping contribution of $Si\text{-}O^-$ stretching vibrations of the various coexisting Q^i silicate tetrahedra (7-9, 11-14). Thus, the spectra of Fig. 1 suggest that the relative abundance of silicate units is a function of boron content. The quantification of this effect requires the deconvolution of the 800-1250 cm^{-1} envelopes, where scattering arises from Q^i silicate units.

Deconvolution of the Raman profiles was done according to standard techniques (15) and the results are shown in Fig. 2. It was found that six bands were adequate to achieve a reasonable agreement between experimental and simulated spectra. These bands can be assigned to Q^i tetrahedra as follows: band 1 (885-862 cm^{-1}) to Q^1, band 2 (960-948 cm^{-1}) to Q^2 and band 4 (1100-1080 cm^{-1}) to Q^3 (11). Bands 5 (1152-1135 cm^{-1}) and 6 (1197-1194 cm^{-1}) are attributed to Q^4 species, i.e. to fully polymerized silicate tetrahedra (11). Band 3 (1065-1040 cm^{-1}) originates from scattering of silicate species containing bridging oxygen atoms, like Q^4 (11) and Q^3, Q^2, Q^1 (14).

The relative intensities of the deconvoluted bands can be subsequently employed to estimate the abundance of silicate tetrahedra. Following Mysen et al (14) the mole fraction X_i of species Q^i (i= 1, 2, 3) with 4-i non-bridging oxygens is given by:

$$X_i = A_i \alpha_i \qquad (3)$$

where A_i is the relative Raman intensity and α_i is the normalized Raman cross section of species Q^i. The values $\alpha_1 = 0.33$, $\alpha_2 = 0.5$ and $\alpha_3 = 1.0$ were used for species Q^1, Q^2 and Q^3,

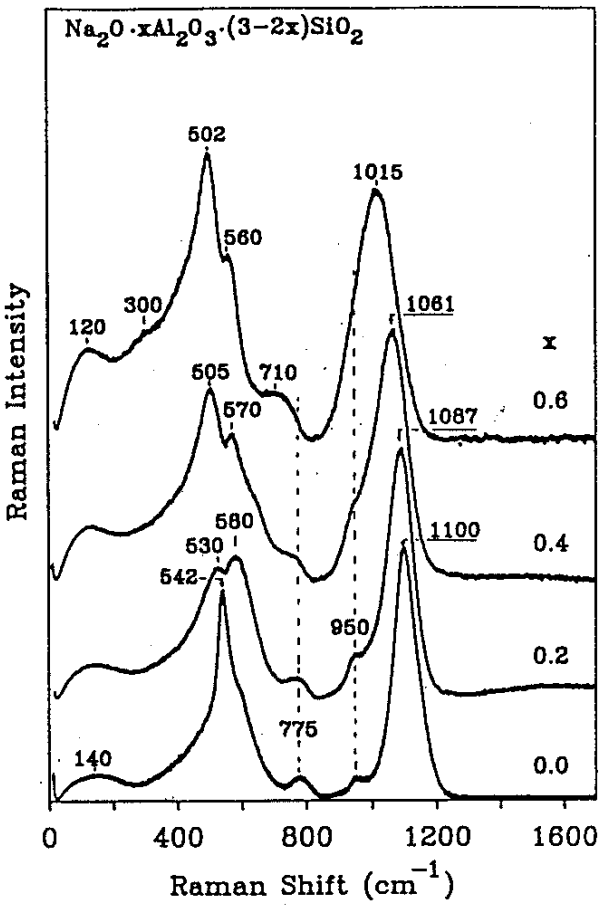

Fig. 4. *Raman spectra of SAS glasses.*

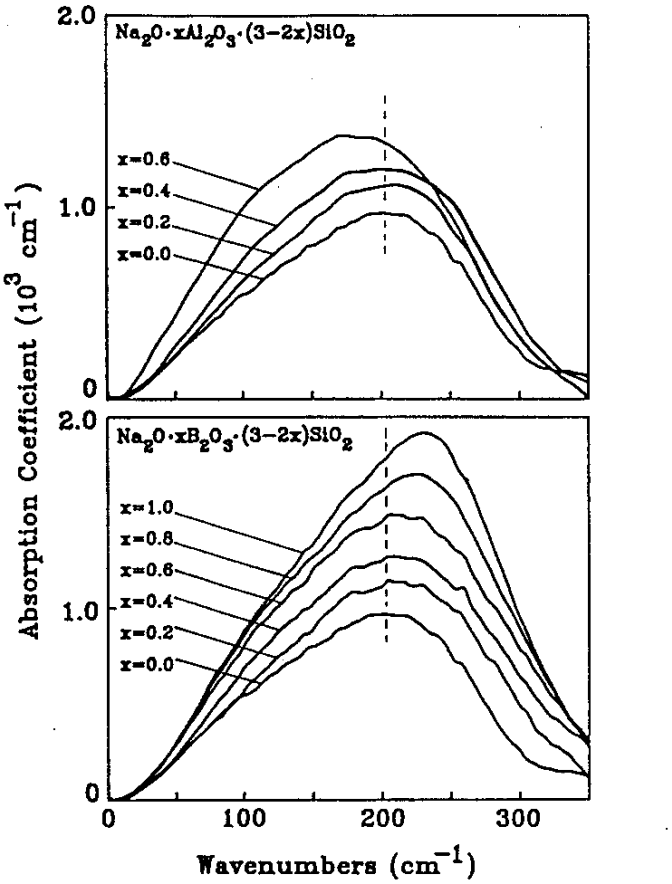

Fig. 5. *Comparison of the effects of boron and aluminum substitution for silicon on the Na^+-motion bands active in the far-infrared*

respectively (14). The mole fraction of Q^4 units is determined from the difference:

$$X_{3D} = 1 - \sum_{i=1}^{3} X_i \qquad (4)$$

The calculated mole fractions of silicate units are shown in Fig. 3 as a function of boron content. It is noted that the results for the sodium trisilicate glass (x=0) agree quite well with those of previous Raman studies (14, 16), as well as those of ^{29}Si NMR measurements (17).

It is quite clear from Fig. 3 that the decrease of the relative abundance of Q^3 species with increasing boron content is accompanied by the increased abundance of Q^2, Q^1 and Q^4 species. It is recalled at this point that additional evidence for the creation of Q^2 and Q^1 species is provided by the development of the lower frequency bands at 630 and 690 cm^{-1} respectively.

The Structure of Sodium-Aluminosilicate Glasses

The Raman spectra of SAS glasses are shown in Fig. 4. As in the case of SBS glasses, the high-frequency envelope between 800 and 1200 cm^{-1} broadens and downshifts with increasing Al content. However, the behaviour of this envelope alone is not very informative for a possible change in the relative abundance of silicate tetrahedra with Al substitution. This is because of the strong coupling of Si-O and Al-O vibrations (18) in mixed alumino-silicate arrangements, $Si-(OAl)_n$ (n= 1-4), in addition to the coexisting Q^i silicate tetrahedra. Nevertheless, inspection of the lower frequency region shows the absence of bands

characteristic of Q^2 (630 cm^{-1}) and Q^1 (690 cm^{-1}) species.

The presence of mixed Si-O-Al bridges is supported by the band developing at ca 500 cm^{-1}, while the feature at 560 cm^{-1} is characteristic of Al-O-Al bridges, where Al is tetrahedrally coordinated (19). The aluminum-oxygen stretching vibration of AlO_4^- tetrahedra is responsible for the band at ca 710 cm^{-1} (20).

It appears from the above that the effect of Al is different from that of B, since neither Q^2 nor Q^1 species are created. Instead, the presence of Si-O-Al bridges suggest that AlO_4^- tetrahedra enter the silicate network and occupy Q^3 sites, i.e. sites of the same formal charge. This is in agreement with the results of XPS (6), molecular dynamics (21) and EXAFS (22) studies.

When Q^3 species are replaced by AlO_4^- tetrahedra the equilibrium,

$$2Q^3 \leftrightarrows Q^2 + Q^4 \qquad (5)$$

is shifted to the left. This process implies that the negative charge becomes more uniformly distributed on the silicate network, when compared to $Na_2O.3SiO_2$ glasses.

Interactions Between Sodium Ions and Their Sites in SAS and SBS glasses

The change in the relative abundance of silicate tetrahedra in the presence of boron affects the distribution of the negative charge on the silicate network. This charge appears to be progressively accumulated on the highly charged Q^2 and Q^1 species upon increasing B content. On the contrary, aluminum was found to favour the homogeneous distribution of negative charge on the glass network. Such changes are expected to affect the charge density of the sites hosting Na^+ ions and thus to influence the Na^+-site interactions. Infrared spectroscopy can be used to probe such effects. This is because the frequency of the Na^+-motion bands, which are active in the infrared, is proportional to an effective charge $q^* = (q_{Na}.q_A)^{1/2}$, where q_{Na}, q_A are the effective charges of sodium ion and network site, respectively (15). While a detailed infrared study will be reported elsewhere (23), Fig. 5 shows the far-infrared regions of the spectra of SBS and SAS glasses. It is observed that the Na^+-motion band shifts to higher frequencies upon B substitution, suggesting a progressive strengthening of the Na^+-site interactions. This trend is opposite to that exhibited by SAS glasses, where the far-infrared envelope shifts eventually to lower frequencies upon increasing Al contents.

A key result of the XPS study of the same glasses (6) was that Na^+ ions are more ionized in SAS than in SBS glasses of the same R/Si ratio (i.e. $q_{Na}(SAS) > q_{Na}(SBS)$). This result combined with the far-infrared behaviour of these glasses suggests that the average charge density of sites hosting Na^+ ions is smaller in SAS than SBS glasses. In terms of the Anderson and Stuart model for ionic conduction (24), the present results would imply a smaller electrostatic energy term for the ion motion activation energy in SAS glasses. In addition, excess volume arguments have suggested that the strain energy term is also smaller in SAS glasses (5). Both terms combined suggest an overall activation energy for ionic conduction smaller in SAS than SBS glasses, as it was found experimentally in previous studies (3-5).

CONCLUSIONS

The study of the Raman and infrared spectra of $Na_2O.R_2O_3.(3-2x)SiO_2$ (R= Al, B) glasses has revealed a number of differences between Al and B substitution for Si. It was found that in the presence of B the silicate network disproportionates to highly charged Q^2 and Q^1 species and to fully polymerized Q^4 tetrahedra at the expense of Q^3 units. Substitution of Si by Al causes the opposite effect, since the equilibrium $2Q^3 \rightleftarrows Q^2+Q^4$ shifts to the left and induces a structural homogenization. Such structural rearrangements affect the distribution

of the negative charge on the glass network and therefore the interactions between Na^+ ions and their sites. These effects are discussed in relation to ion conduction properties exhibited by these glasses.

Support for this work was provided by NSF, NHRF and the Humbolt Foundation

REFERENCES

1. D. E. Day and G. E. Rindone, J. Am. Ceram. Soc. 45 (1962) 489 ; 45 (1962) 496
2. J. O. Isard, J. Soc. Glass Technol. 43 (1959) 113
3. K. Otto, Phys. Chem. Glasses 7 (1966) 29
4. H. Wakabayashi, Phys. Chem. Glasses 30 (1989) 51
5. H. Jain and C. H. Hsieh, in: Physics of Non-Crystalline Solids, eds. L. D. Pye, W. C. LaCourse and H. J. Stevens (Taylor & Francis, London 1992) p. 447.
6. C. H. Hsieh, H. Jain, A. C. Miller and E. I. Kamitsos, J. Non-Cryst. Solids, in press
7. S. A. Brawer and W. B. White, J. Chem. Phys. 63 (1975) 2421
8. T. Furukawa, K. E. Fox and W. B. White, J. Chem. Phys. 75 (1981) 3226
9. T. Furukawa and W. B. White, J. Non-Cryst. Solids 38-39 (1980) 87
10. E. I. Kamitsos, M. A. Karakassides and G. D. Chryssikos, Phys. Chem. Glasses 28 (1987) 203; 30 (1989) 19
11. P. McMillan, Am. Mineral. 69 (1984) 622
12. N. Umesaki, N. Iwamoto, T. Tatsumisago and T. Minami, J. Non-Cryst. Solids 106 (1988) 77
13. F. Domine and B. Piriou, Am. Mineral. 71 (1986) 38
14. B. O. Mysen, D. Virgo and F. A. Seifert, Am. Mineral. 70 (1985) 88
15. E. I. Kamitsos, A. P. Patsis and G. D. Chryssikos, J. Non-Cryst. Solids 126 (1990) 52; 152 (1993) 246
16. B. O. Mysen, Am. Mineral. 75 (1990) 120
17. H. Maekawa, T. Maekawa, K. Kawamura and T. Yokokawa, J. Non-Cryst. Solids 127 (1991) 53
18. F. Gervais, C. Lagrange, A. Blin, M. Aliari, G. Hauret, J. P. Coutures and M. Leroux, J. Non-Cryst. Solids 119 (1990) 79
19. P. McMillan, B. Piriou and A. Navrotsky, Geochim. Cosmochim. Acta 46 (1982) 2021
20. P. McMillan and B. Piriou, J. Non-Cryst. Solids 53 (1982) 279; 55 (1983) 221
21. D. M. Zirl and S. H. Garofalini, J. Am. Ceram. Soc. 73 (1990) 2848
22. D. A. McKeon, G. A. Waychunas and G. E. Brown, J. Non-Cryst. Solids 74 (1985) 349
23. E. I. Kamitsos, J. A. Kapoutsis, H. Jain and C. H. Hsieh, J. Non-Cryst. Solids, in press
24. O. L. Anderson and D. A. Stuart, J. Am. Ceram. Soc. 37 (1954) 573